Heredity (2008) 100, 326–336

www.nature.com/hdy

ORIGINAL ARTICLE

Differential barrier strength and allele frequencies in hybrid zones maintained by sex-biased hybrid incompatibilities

R-X Wang and Y-L Zhao
BC Cancer Research Centre, BC Cancer Agency, Vancouver, British Columbia, Canada

In animals, hybrid sterility and inviability between closely related species often affect only the heterogametic sex (*XY*). This widespread phenomenon, known as Haldane's rule, is an early speciation event found across broad taxa, but the role of heterogametic hybrid incompatibilities, as opposed to homogametic ones, as a barrier in a speciation process remains obscure. It has been hypothesized that heterogametic incompatibility may be a more efficient mechanism in driving speciation. The population dynamics after (rather than before) the occurrence of sex-biased incompatibilities may account for Haldane's rule. In this study, a recursion model of hybrid zones was developed to investigate the differences between heterogametic and homogametic incompatibilities. The selection strengths and selection patterns of sex chromosome-linked, two-locus Bateson–Dobzhansky–Muller (BDM) genetic incompatibilities were examined. It is noted that a sex-biased hybrid incompatibility in a hybrid zone confers asymmetric and uneven impedance to gene flow. The clines of different loci in such a hybrid zone displayed diverse differentiation in their width, steepness and asymmetry. Alleles involved in the incompatibility face much stronger resistance to cross a hybrid zone. Different sex-biased BDM incompatibilities also affect the flow of neutral alleles differently. Compared to a homogametic one, heterogametic incompatibility is a weaker but more asymmetric barrier. These unique patterns of gene flow may explain uneven divergence among different genomic regions during speciation between some closely related species.
Heredity (2008) **100,** 326–336; doi:10.1038/sj.hdy.6801081; published online 19 December 2007

Keywords: fitness; genetic load; Haldane's rule; gene flow; sex-biased incompatibility; hybrid zone

Introduction

In animals, when the F_1 hybrid of a particular gender between closely related species is sterile or inviable, it is almost always the heterogametic sex (Haldane, 1922). This generalization, known as Haldane's rule, applies to both male heterogametic (*XY* or *XO*, as in mammals and some insects) and female heterogametic (*ZW*, as in birds and lepidopterans) species (Coyne and Orr, 1989; Wu and Davis, 1993; Laurie, 1997). Clearly, Haldane's rule is a phenomenon that is associated with the heterogametic genotype in which the sex chromosome-linked alleles are hemizygous. The mechanism underlying this association has been a puzzling problem. Numerous attempts have been made in searching for a general genetic basis for Haldane's rule, but none of the mechanisms identified could explain the generality of the rule. Without a plausible general genetic basis, 'the composite notion' was proposed, which subdivides Haldane's rule and employs various explanations for the different divisions (Wu and Davis, 1993; Orr, 1993a). Haldane's rule now appears to be a 'solved' problem under the composite notion (see Turelli, 1998).

We view Haldane's rule from a different perspective. Studies so far have mainly focused on how heterogametic hybrid incompatibilities arise and whether or not they do occur more often than homogametic ones. Little attention has been paid to the role of heterogametic incompatibilities (as opposed to rarely found homogametic incompatibilities) as a driving force of speciation, namely, its effects on gene flow as isolating barriers (Wang, 2003). We ask how a sex-biased hybrid incompatibility affects gene flow and genetic divergence, after it arises. Provided that a heterogametic incompatibility had the same rate of occurrence during evolution as that of a homogametic one, would population dynamics make the heterogametic incompatibility more visible or more preserved?

Decades of explorations have demonstrated that heterogametic F_1 hybrid inferiority can be caused by various forms of genetic incompatibilities. These include chromosomal rearrangements of the sex chromosomes (Haldane, 1932), *X*-linked recessive defects (the dominance theory; see Dobzhansky, 1937; Muller, 1940, 1942; Orr, 1993b; Turelli and Orr, 1995, 2000), dosage compensation (Cline and Meyer, 1996), *X*–*Y* incompatibilities (Muller, 1942; White, 1945; Heikkinen and Lumme, 1998), *Y*–autosomal incompatibilities (Pantazidis and Zouros, 1988; Pantazidis *et al*., 1993; Heikkinen and

Correspondence: Dr R-X Wang, BC Cancer Research Centre, BC Cancer Agency, 675 W 10th Avenue, Vancouver, British Columbia, Canada V5Z 1L3.
E-mail: rwang@bccrc.ca
Received 15 December 2006; revised 26 October 2007; accepted 6 November 2007; published online 19 December 2007

Lumme, 1998) and meiotic drive (Frank, 1991; Hurst and Pomiankowski, 1991). All these mechanisms have little in common, except that they are always sex chromosome-linked and only affect hybrids of the heterogametic sex (see reviews of Coyne and Orr, 1989; Laurie, 1997). Also, they all operate as epistatic Bateson–Dobzhansky–Muller (BDM) incompatibilities—the involved alleles are incompatible with each other when coexisting in hybrids but fully fit in the respective parental genomes.

Previously, Wang (2003) developed an introgression model to examine such sex-biased BDM isolation in allopatry. It was revealed that the ability of sex-biased hybrid incompatibilities to impede gene flow varies according to the sex affected and the chromosome involved. Heterogametic and homogametic hybrid incompatibilities are not equivalent isolating barriers. Heterogametic incompatibility displays differential strength on introgression of different alleles. Heterogametic incompatibility confers stronger asymmetric introgression and is a more diverse and, perhaps, a more efficient isolating mechanism against introgression (Wang, 2003). However, it is difficult to test the introgression model in empirical investigations. This model does not apply to the parapatric system, which is an active area for both theoretical and empirical studies.

In parapatry, two populations are in direct contact and a boundary hybrid zone is present. Studying sex-biased BDM incompatibilities in the scenarios of parapatry may help fill the gaps between theories and empirical studies. The dynamics of gene flow in tension zones, namely a hybrid zone under genetic selection, is mainly determined by the strength of genetic selection and dispersal (Barton and Bengtsson, 1986). The existing theoretical framework of tension zone study has been mainly developed to address nonsex-related barriers. They are founded on the Hardy–Weinberg equation, which assumes equal passage of alleles from both sexes between generations (Endler, 1973; Slatkin, 1973; Nagylaki, 1975; Barton, 1979, 1986; Gavrilets, 1997). These models are not applicable to cases with sex-biased hybrid incompatibilities. An analysis of the genetic dynamics in a tension zone maintained by sex-biased BDM type postzygotic isolation may thus provide novel insights into the mechanism of speciation and facilitate empirical studies.

In this study, a generation-by-generation recursion model was developed to evaluate the strength of sex-biased hybrid incompatibilities in impeding gene flow across a hybrid zone. We modeled a two-locus BDM incompatibility that is linked to at least one sex-chromosomal allele. We have two purposes. The first is to define the properties of a sex-biased BDM incompatibility as a barrier in tension zones. The sex-biased and sex chromosome-linked BDM incompatibilities have not been addressed by existing hybrid zone models (Endler, 1973; Slatkin, 1973; Nagylaki, 1975; Barton, 1979, 1986; Gavrilets, 1997). We hope to delineate how such genetic selection could shape tension zone structures and dynamics. Our second purpose is to identify the unique characteristics of heterogametic incompatibilities in a tension zone as opposed to homogametic ones. Such characteristics may provide insights into the hybrid zone dynamics and help explain the mechanism underlying Haldane's rule (Wang, 2003). Genetic load, allele frequencies and departure of genotype distributions from the Hardy–Weinberg equilibrium across a tension zone were examined. The analysis starts from modeling a simplified, static hybridizing deme that only receives inputs once, to show the intrinsic selection of sex-biased BDM isolation. The model is then extended to more dynamic scenarios, that is, hybrid zones maintained by a sex-biased BDM incompatibility, and long- or short-range dispersal.

Model

Sex-biased inferiority, which is caused by a two-locus BDM incompatibility, was mainly considered. Briefly, two closely related diploid populations (conspecific populations, H_1 and H_2 in the text) derived from a common ancestor evolve a genetic incompatibility between one allele from H_1 and another allele from H_2 that causes sterility or inviability in one sex. The incompatible alleles are located on different chromosomes. All other alleles are neutral in fitness and fully compatible with each other, except for the ones involved in an incompatibility. Thus, hybrids of the affected sex carrying the incompatible genotype are unfit and will be eliminated, but all other progeny are equally fit. The unaffected progeny are subject to further segregation and random mating in later generations.

It was assumed that in a closed habitat or independent niche, individuals from two diverging populations, H_1 and H_2, mix to form an independent deme. Random mating, discrete/nonoverlapping generations and the passage of alleles into the next generation at their probabilities were assumed. In this model, five independently localized loci each with two alleles are considered, denoted X_1/X_2, Y_1/Y_2, A_1/A_2, B_1/B_2 and C_1/C_2 from either H_1 or H_2, in which X or Y represents an X or Y chromosome-linked locus, and A, B or C is an autosomal locus. The genotypes of individuals from H_1 are $X_1X_1A_1A_1B_1B_1C_1C_1$ for females and $X_1Y_1A_1A_1B_1B_1C_1C_1$ for males; from H_2 the genotypes are $X_2X_2A_2A_2B_2B_2C_2C_2$ for females and $X_2Y_2A_2A_2B_2B_2C_2C_2$ for males. All these genotypes are expressed as $X_iX_jA_kA_lB_mB_nC_oC_p$ for females and $X_iY_jA_kA_lB_mB_nC_oC_p$ for males, where i, j, k, l, m, n, o or p is either 1 or 2. Therefore, there are $2^8 = 256$ possible genotypic combinations of offspring for each sex (bear in mind that not all these combinations represent independent genotypes). The genotypic combinations and their probabilities can be calculated accordingly. For instance, the genotypes (and their probabilities) of male offspring in the first generation of equal mixing are $X_1Y_1A_1A_1B_1B_1C_1C_1$ (0.25), $X_1Y_2A_1A_2B_1B_2C_1C_2$ (0.25), $X_2Y_1A_1A_2B_1B_2C_1C_2$ (0.25) or $X_2Y_2A_2A_2B_2B_2C_2C_2$ (0.25). Those of female offspring are $X_1X_1A_1A_1B_1B_1C_1C_1$ (0.25), $X_1X_2A_1A_2B_1B_2C_1C_2$ (0.5) or $X_2X_2A_2A_2B_2B_2C_2C_2$ (0.25).

We consider multigenerational effects in the model. When a BDM incompatibility arises between two parapatric populations, admixture of migrants in a hybridizing deme would lead to the production of inferior hybrid offspring in multiple generations. Such a multigenerational effect is a default property of BDM type isolation and its presence in cases following Haldane's rule has been confirmed (Wu and Davis, 1993).

The probability of a genotype of a sperm or an egg in any generation t can be computed by

$$p^{(t)_{\text{sperm}}}_{X_rA_tB_vC_z} = \frac{\sum_{i=1}^{2}\sum_{k=1}^{2}\sum_{l=1}^{2}\sum_{m=1}^{2}\sum_{n=1}^{2}\sum_{o=1}^{2}\sum_{p=1}^{2}[C_{X_rA_tB_vC_z}(j,k,l,m,n,o,p)((1-\lambda)N^{(t)}p^{(t)}_{X_rY_jA_kA_lB_mB_nC_oC_p} + \lambda N^0 p^0_{X_rY_jA_kA_lB_mB_nC_oC_p})]}{\sum_{i=1}^{2}\sum_{j=1}^{2}\sum_{k=1}^{2}\sum_{l=1}^{2}\sum_{m=1}^{2}\sum_{n=1}^{2}\sum_{o=1}^{2}\sum_{p=1}^{2}((1-\lambda)N^{(t)}p^{(t)}_{X_iY_jA_kA_lB_mB_nC_oC_p} + \lambda N^0 p^0_{X_iY_jA_kA_lB_mB_nC_oC_p})}$$
$$= \frac{\sum_{i=1}^{2}\sum_{k=1}^{2}\sum_{l=1}^{2}\sum_{m=1}^{2}\sum_{n=1}^{2}\sum_{o=1}^{2}\sum_{p=1}^{2}[C_{X_rA_tB_vC_z}(j,k,l,m,n,o,p)((1-\lambda)N^{(t)}p^{(t)}_{X_rY_jA_kA_lB_mB_nC_oC_p} + \lambda N^0 p^0_{X_rY_jA_kA_lB_mB_nC_oC_p})]}{(1-\lambda)N^{(t)} + \lambda N^0} \quad (1)$$

$$p^{(t)_{\text{sperm}}}_{Y_rA_tB_vC_z} = \frac{\sum_{i=1}^{2}\sum_{k=1}^{2}\sum_{l=1}^{2}\sum_{m=1}^{2}\sum_{n=1}^{2}\sum_{o=1}^{2}\sum_{p=1}^{2}[D_{Y_rA_tB_vC_z}(i,k,l,m,n,o,p)((1-\lambda)N^{(t)}p^{(t)}_{X_iY_rA_kA_lB_mB_nC_oC_p} + \lambda N^0 p^0_{X_iY_rA_kA_lB_mB_nC_oC_p})]}{\sum_{i=1}^{2}\sum_{j=1}^{2}\sum_{k=1}^{2}\sum_{l=1}^{2}\sum_{m=1}^{2}\sum_{n=1}^{2}\sum_{o=1}^{2}\sum_{p=1}^{2}((1-\lambda)N^{(t)}p^{(t)}_{X_iY_jA_kA_lB_mB_nC_oC_p} + \lambda N^0 p^0_{X_iY_jA_kA_lB_mB_nC_oC_p})}$$
$$= \frac{\sum_{i=1}^{2}\sum_{k=1}^{2}\sum_{l=1}^{2}\sum_{m=1}^{2}\sum_{n=1}^{2}\sum_{o=1}^{2}\sum_{p=1}^{2}[D_{Y_rA_tB_vC_z}(i,k,l,m,n,o,p)((1-\lambda)N^{(t)}p^{(t)}_{X_iY_rA_kA_lB_mB_nC_oC_p} + \lambda N^0 p^0_{X_iY_rA_kA_lB_mB_nC_oC_p})]}{(1-\lambda)N^{(t)} + \lambda N^0} \quad (2)$$

$$p^{(t)_{\text{egg}}}_{X_qA_sB_uC_w} = \frac{\sum_{i=1}^{2}\sum_{j=1}^{2}\sum_{k=1}^{2}\sum_{l=1}^{2}\sum_{m=1}^{2}\sum_{n=1}^{2}\sum_{o=1}^{2}\sum_{p=1}^{2}[E_{X_qA_sB_uC_w}(i,j,k,l,m,n,o,p)((1-\lambda)N^{(t)}p^{(t)}_{X_iX_jA_kA_lB_mB_nC_oC_p} + \lambda N^0 p^0_{X_iX_jA_kA_lB_mB_nC_oC_p})]}{\sum_{i=1}^{2}\sum_{j=1}^{2}\sum_{k=1}^{2}\sum_{l=1}^{2}\sum_{m=1}^{2}\sum_{n=1}^{2}\sum_{o=1}^{2}\sum_{p=1}^{2}((1-\lambda)N^{(t)}p^{(t)}_{X_iX_jA_kA_lB_mB_nC_oC_p} + \lambda N^0 p^0_{X_iX_jA_kA_lB_mB_nC_oC_p})}$$
$$= \frac{\sum_{i=1}^{2}\sum_{j=1}^{2}\sum_{k=1}^{2}\sum_{l=1}^{2}\sum_{m=1}^{2}\sum_{n=1}^{2}\sum_{o=1}^{2}\sum_{p=1}^{2}[E_{X_qA_sB_uC_w}(i,j,k,l,m,n,o,p)((1-\lambda)N^{(t)}p^{(t)}_{X_iX_jA_kA_lB_mB_nC_oC_p} + \lambda N^0 p^0_{X_iX_jA_kA_lB_mB_nC_oC_p})]}{(1-\lambda)N^{(t)} + \lambda N^0} \quad (3)$$

where q, r, s, t, u, v, w or z equals 1 or 2 and λ is the dispersal rate, which ranges from 0 to 0.5. C, D and E are the coefficients (Tables 1 and 2) for producing sperms with X, sperms with Y and eggs, respectively, from a mature individual of either sex with certain genotypes. The $N^{(t)}$ is the deme size and N^0 is the size of the founding deme at generation 0. It is obvious that $N^{(t)} \leqslant N^0$ because only deleterious selection is considered in the model.

Accordingly, the probability of a given genotype in generation t in a hybridizing deme is the combination of that of a sperm and an egg,

$$p^{(t)}_{X_qX_rA_sA_tB_uB_vC_wC_z} = p^{(t-1)_{\text{egg}}}_{X_qA_sB_uC_w} \cdot p^{(t-1)_{\text{sperm}}}_{X_rA_tB_vC_z} \quad (4)$$

or

$$p^{(t)}_{X_qY_rA_sA_tB_uB_vC_wC_z} = p^{(t-1)_{\text{egg}}}_{X_qA_sB_uC_w} \cdot p^{(t-1)_{\text{sperm}}}_{Y_rA_tB_vC_z} \quad (5)$$

where $p^{(t)}_{X_qX_rA_sA_tB_uB_vC_wC_z}$ or $p^{(t)}_{X_qY_rA_sA_tB_uB_vC_wC_z}$ stands for the probability of a genotype $X_qX_rA_sA_tB_uB_vC_wC_z$ or $X_qY_rA_sA_tB_uB_vC_wC_z$ in females or males, respectively, in generation t.

Equations (1)–(5) can be used to calculate the probabilities of gametes and offspring of each genotype in any generation with ($\lambda > 0$) or without dispersal ($\lambda = 0$). For instance, for sperm or egg with genotype $X_1A_1C_1$ in generation t, it is, respectively,

Table 1 Genotypic coefficients (C or D) for producing sperms

$X_iY_jA_kA_lB_mB_nC_oC_p$	$C_{X_rA_tB_vC_z}(j,k,l,m,n,o,p)$ $(i=r)$	$D_{Y_rA_tB_vC_z}(i,k,l,m,n,o,p)$ $(j=r)$
$k=l=t$; $m=n=v$; $o=p=z$	1/2	1/2
$k=l=t$; $m=n=v$; $o\neq p$ and (o or $p=z$)	1/4	1/4
$k=l=t$; $m\neq n$ and (m or $n=v$); $o=p=z$	1/4	1/4
$k=l=t$; $m\neq n$ and (m or $n=v$); $o\neq p$ and (o or $p=z$)	1/8	1/8
$k\neq l$ and (k or $l=t$); $m=n=v$; $o=p=z$	1/4	1/4
$k\neq l$ and (k or $l=t$); $m=n=v$; $o\neq p$ and (o or $p=z$)	1/8	1/8
$k\neq l$ and (k or $l=t$); $m\neq n$ and (m or $n=v$); $o=p=z$	1/8	1/8
$k\neq l$ and (k or $l=t$), $m\neq n$ and (m or $n=v$); $o\neq p$ and (o or $p=z$)	1/16	1/16
Others	0	0

Table 2 Genotypic coefficients (E) for producing eggs

$X_iX_jA_kA_lB_mB_nC_oC_p$	$E_{X_qA_sB_uC_w}(i,j,k,l,m,n,o,p)$
$i=j=q$; $k=l=s$; $m=n=u$; $o=p=w$	1
$i=j=q$; $k=l=s$; $m=n=u$; $o\neq p$ and (o or $p=w$)	1/2
$i=j=q$; $k=l=s$; $m\neq n$ and (m or $n=u$); $o=p=w$	1/2
$i=j=q$; $k=l=s$; $m\neq n$ and (m or $n=u$); $o\neq p$ and (o or $p=w$)	1/4
$i=j=q$; $k\neq l$ and (k or $l=s$); $m=n=u$; $o=p=w$	1/2
$i=j=q$; $k\neq l$ and (k or $l=s$); $m=n=u$; $o\neq p$ and (o or $p=w$)	1/4
$i=j=q$; $k\neq l$ and (k or $l=s$); $m\neq n$ and (m or $n=u$); $o=p=w$	1/4
$i=j=q$; $k\neq l$ and (k or $l=s$); $m\neq n$ and (m or $n=u$); $o\neq p$ and (o or $p=w$)	1/8
$i\neq j$ and (i or $j=q$); $k=l=s$; $m=n=u$; $o=p=w$	1/2
$i\neq j$ and (i or $j=q$); $k=l=s$; $m=n=u$; $o\neq p$ and (o or $p=w$)	1/4
$i\neq j$ and (i or $j=q$); $k=l=s$; $m\neq n$ and (m or $n=u$); $o=p=w$	1/4
$i\neq j$ and (i or $j=q$); $k=l=s$; $m\neq n$ and (m or $n=u$); $o\neq p$ and (o or $p=w$)	1/8
$i\neq j$ and (i or $j=q$); $k\neq l$ and (k or $l=s$); $m\neq n$ and (m or $n=u$); $o=p=w$	1/8
$i\neq j$ and (i or $j=q$); $k\neq l$ and (k or $l=s$); $m\neq n$ and (m or $n=u$); $o\neq p$ and (o or $p=w$)	1/16
Others	0

$$p^{(t)_{\text{sperm}}}_{X_1A_1B_1C_1}=\frac{\sum_{i=1}^{2}\sum_{k=1}^{2}\sum_{l=1}^{2}\sum_{m=1}^{2}\sum_{n=1}^{2}\sum_{o=1}^{2}\sum_{p=1}^{2}[C_{X_1A_1B_1C_1}(i,k,l,m,n,o,p)\cdot((1-\lambda)N^{(t)}p^{(t)}_{X_1Y_iA_kA_lB_mB_nC_oC_p}+\lambda N^0p^0_{X_1Y_iA_kA_lB_mB_nC_oC_p})]}{(1-\lambda)N^{(t)}+\lambda N^0}$$

or

$$p^{(t)_{\text{egg}}}_{X_1A_1B_1C_1}=\frac{\sum_{i=1}^{2}\sum_{j=1}^{2}\sum_{k=1}^{2}\sum_{l=1}^{2}\sum_{m=1}^{2}\sum_{n=1}^{2}\sum_{o=1}^{2}\sum_{p=1}^{2}[E_{X_1A_1B_1C_1}(i,j,k,l,m,n,o,p)\cdot((1-\lambda)N^{(t)}p^{(t)}_{X_1X_iA_kA_lB_mB_nC_oC_p}+\lambda N^0p^0_{X_1X_iA_kA_lB_mB_nC_oC_p})]}{(1-\lambda)N^{(t)}+\lambda N^0}$$

Similarly, the probability of the genotype of $X_1X_1A_1A_1B_1B_1C_1C_1$ in the generation t is

$$p^{(t)}_{X_1X_1A_1A_1B_1B_1C_1C_1}=p^{(t-1)_{\text{egg}}}_{X_1A_1B_1C_1}\cdot p^{(t-1)_{\text{sperm}}}_{X_1A_1B_1C_1}$$

In a hybrid zone, when individuals from both populations mix to form an interbreeding deme, the BDM incompatibility will be expressed and incompatible alleles constitute genetic load. Genetic load in this scenario is different from a scenario in which each allele is under direct selection independently. To evaluate such fitness effects or barrier strength of a BDM incompatibility, modified definitions of deme fitness ($W^{(t)}$) and genetic load ($L^{(t)}$) are adopted here. The $W^{(t)}$ is defined as the deme size in generation t divided by the size of the founding deme ($W^{(t)}=N^{(t)}/N^0$). The $L^{(t)}$ is the total amount of inferior offspring produced up to generation t divided by the size of the founding deme. In other words, the $L^{(t)}$ is the eliminated fraction of a closed deme (because of incompatibility) within generation t divided by the size of an otherwise equivalent deme unaffected by incompatibility. The genetic load used here takes account of accumulative effects over multiple generations and is different from the barrier strength considered by Bengtsson (1985), Barton and Bengtsson (1986) and Gavrilets (1997) that only considers F_1 hybrids.

With these assumptions, the probability of any genotype in generation t can be computed.

In generation t, the mean fitness loss from generation $(t-1)$ to t is

$$d^{(t)}=W^{(t-1)}\cdot\Delta p^{(t)}\cdot N^0/N^0=W^{(t-1)}\cdot\Delta p^{(t)} \tag{6}$$

where $\Delta p^{(t)}$ represents the probability of inferior offspring. For instance, in the case of an X_rA_s heterogametic incompatibility, the probability of inferior offspring in generation t is

$$\Delta p^{(t)}=\sum_{j=1}^{2}\sum_{k=1}^{2}\sum_{l=1}^{2}\sum_{m=1}^{2}\sum_{n=1}^{2}\sum_{o=1}^{2}\sum_{p=1}^{2}[p^{(t)}_{X_rY_jA_sA_lB_mB_nC_oC_p}+p^{(t)}_{X_rY_jA_kA_sB_mB_nC_oC_p}-p^{(t)}_{X_rY_jA_sA_sB_mB_nC_oC_p}].$$

The deme fitness $W^{(t)}$ relative to $(t=0)$ is

$$W^{(t)}=W^{(t-1)}-d^{(t)}=W^{(t-1)}(1-\Delta p^{(t)})=\prod_1^t(1-\Delta p^{(t)}) \tag{7}$$

Therefore, the genetic load ($L^{(t)}$) of a deme in generation t is

$$L^{(t)}=W^0-W^{(t)}=1-W^{(t)}=1-\prod_1^t(1-\Delta p^{(t)}) \tag{8}$$

In each generation, after elimination of the inferior genotypes, the relative frequencies of other genotypes will change accordingly and will have to be normalized. For instance, in the case of an X_rA_s heterogametic incompatibility with dispersal, the probability of sperm containing X_r (Equation (1)) can be computed using the following equation:

$$p^{(t)_{\text{sperm}}}_{X_rA_tB_vC_z}=\frac{\sum_{j=1}^{2}\sum_{k=1}^{2}\sum_{l=1}^{2}\sum_{m=1}^{2}\sum_{n=1}^{2}\sum_{o=1}^{2}\sum_{p=1}^{2}[C_{X_rA_tB_vC_z}(j,k,l,m,n,o,p)((1-\lambda)N^{(t)}p^{(t)}_{X_rY_jA_kA_lB_mB_nC_oC_p}+\lambda N^0p^0_{X_rY_jA_kA_lB_mB_nC_oC_p})]}{(1-\lambda-\Delta p^{(t)})N^{(t)}+\lambda N^0} \tag{9}$$

The frequency of an allele is the sum of all gametes containing that allele. For instance, the frequency of X_r in the mixed deme in generation t in the presence of X_rA_s incompatibility is the sum of all gametes containing an X_r allele,

$$P_{X_r}^{(t)} = \frac{1}{2}\left(\frac{\sum_{j=1}^{2}\sum_{k=1}^{2}\sum_{l=1}^{2}\sum_{m=1}^{2}\sum_{n=1}^{2}\sum_{o=1}^{2}\sum_{p=1}^{2}[C_{X_rA_tB_vC_z}(j,k,l,m,n,o,p)((1-\lambda)N^{(t)}\cdot p^{(t)}_{X_rY_jA_kA_lB_mB_nC_oC_p}+\lambda N^0 p^0_{X_rY_jA_kA_lB_mB_nC_oC_p})]}{(1-\lambda-\Delta p^{(t)})N^{(t)}+\lambda N^0}\right.$$
$$\left.+\frac{\sum_{i=1}^{2}\sum_{j=1}^{2}\sum_{k=1}^{2}\sum_{l=1}^{2}\sum_{m=1}^{2}\sum_{n=1}^{2}\sum_{o=1}^{2}\sum_{p=1}^{2}[E_{X_rA_sB_uC_w}(i,j,k,l,m,n,o,p)\cdot p^{(t)}_{X_iX_jA_kA_lB_mB_nC_oC_p}+\lambda N^0 p^0_{X_iX_jA_kA_lB_mB_nC_oC_p})]}{(1-\lambda-\Delta p^{(t)})N^{(t)}+\lambda N^0}\right)$$
$$=\frac{1}{2}\left(\frac{\sum_{j=1}^{2}\sum_{k=1}^{2}\sum_{l=1}^{2}\sum_{m=1}^{2}\sum_{n=1}^{2}\sum_{o=1}^{2}\sum_{p=1}^{2}[C_{X_rA_tB_vC_z}(j,k,l,m,n,o,p)((1-\lambda)N^{(t)}\cdot p^{(t)}_{X_rY_jA_kA_lB_mB_nC_oC_p}+\lambda N^0 p^0_{X_rY_jA_kA_lB_mB_nC_oC_p})]}{(1-\lambda-\Delta p^{(t)})N^{(t)}+\lambda N^0}\right.$$
$$\left.+\frac{\sum_{i=1}^{2}\sum_{j=1}^{2}\sum_{k=1}^{2}\sum_{l=1}^{2}\sum_{m=1}^{2}\sum_{n=1}^{2}\sum_{o=1}^{2}\sum_{p=1}^{2}\left[E_{X_rA_sB_uC_w}(i,j,k,l,m,n,o,p)((1-\lambda)N^{(t)}\cdot p^{(t)}_{X_iX_jA_kA_lB_mB_nC_oC_p}+\lambda N^0 p^0_{X_iX_jA_kA_lB_mB_nC_oC_p})\right]}{(1-\lambda-\Delta p^{(t)})N^{(t)}+\lambda N^0}\right) \quad (10)$$

where C and E are the coefficients of different genotypes of both sexes and are given in Tables 1 and 2.

The calculation and graphics used in the figures were generated with MATLAB (The MathWorks Inc., Novi, MI, USA).

Results

To delineate the differentiation between heterogametic and homogametic hybrid incompatibilities, we first examine hybridizing demes where migrants from both parental populations mix once and then evolve independently with zero input. The genetic dynamics of such a closed deme is determined only by the genetic structure and represents the intrinsic strength of an incompatibility. In the later part of the paper, such demes will be placed in the context of hybrid zones and dispersal will be considered. Because X chromosome–autosome (X–A) incompatibilities are the most prevalent form of sex-biased postzygotic isolation (Coyne and Orr, 1989; Wu and Davis, 1993; Laurie, 1997; Heikkinen and Lumme, 1998), we begin with X–A incompatibilities. In this comparison, the genetic compositions of the compared scenarios are the same, except for the sex affected. The analysis will be extended to other forms of two-locus incompatibilities, that is, X–Y, Y–autosomal, X–X, autosomal–autosomal incompatibilities, and compound sex-biased incompatibilities.

To demonstrate the intrinsic selection strength of a unidirectional X–A heterogametic incompatibility and homogametic incompatibility, we first examined the genetic load (L) (Figure 1a) in a deme where H_1 and H_2 are equally mixed (Equation (8)). Here, L is an indicator to show how much a BDM incompatibility alone can affect fitness or the barrier strength (Barton, 1980, 1986; Bengtsson, 1985). Figure 1a shows L under a unidirectional, sex-biased hybrid X_1A_2 incompatibility. The comparison indicates that the L of an equally mixed deme is equilibrated at 0.867 when the heterogametic sex is affected and at 0.982 when the homogametic sex

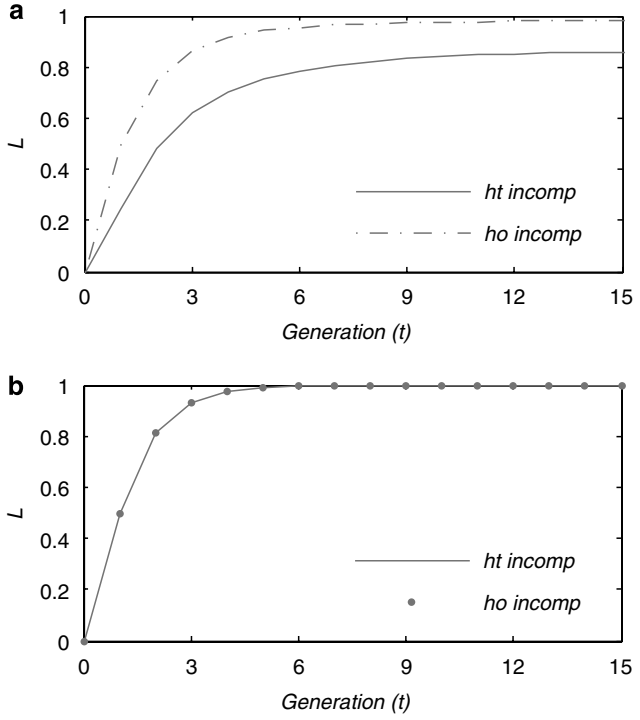

Figure 1 Effects of X_1A_2 unidirectional sex-biased incompatibility on genetic load (L) in a deme that receives 0.5:0.5 contributions from parental populations (H_1:H_2). (**a**) A scenario under an X_1A_2 unidirectional sex-biased incompatibility. The L is relative to the initial fitness ($W^{(0)}=1$) of the deme, in which $L\approx0.867$ for a heterogametic incompatibility and $L\approx0.982$ for a homogametic incompatibility. (**b**) A scenario under compound ($X_1A_2+X_2B_1$) bidirectional sex-biased incompatibilities in which $L\approx0.999621$ for a compound heterogametic incompatibility and $L\approx0.999889$ for a compound homogametic incompatibility. *ht incomp*, heterogametic incompatibility; *ho incomp*, homogametic incompatibility.

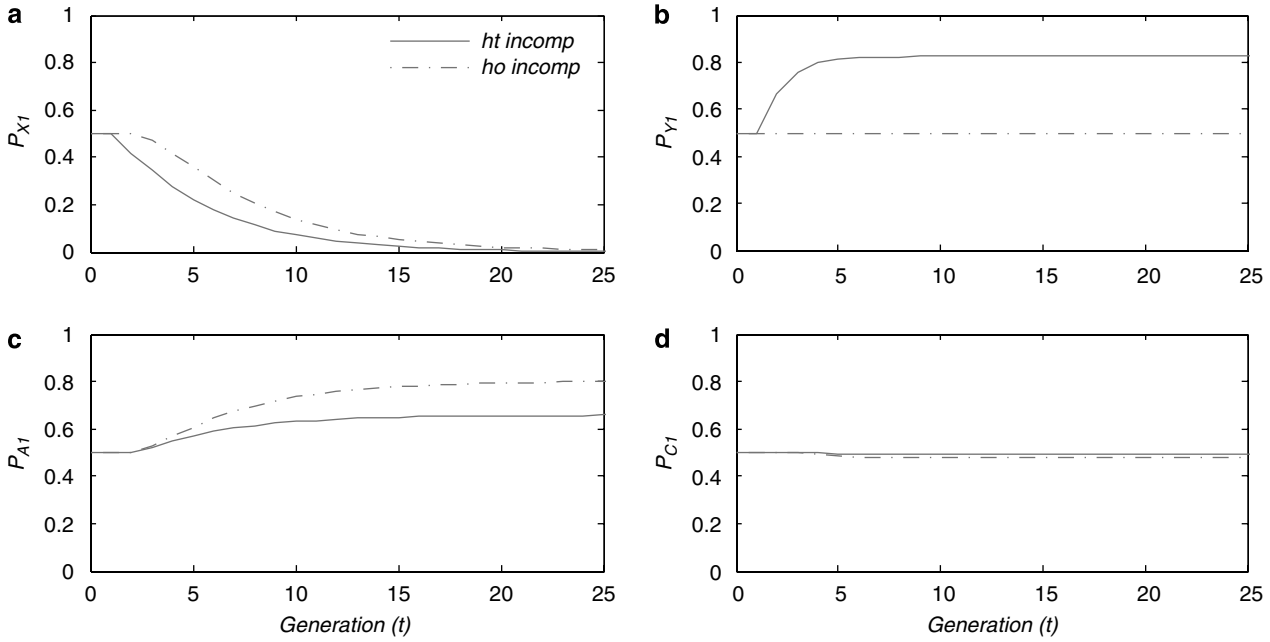

Figure 2 The change of relative allele frequencies (P) in a 0.5:0.5 (H_1:H_2) mixed deme in the presence of an X_1A_2 unidirectional sex-biased incompatibility. Panels **a–d** present the allele frequencies of X_1, Y_1, A_1 and C_1, respectively, in different generations. Here, B locus is not involved in the incompatibility and thus B_1 would behave like the C_1 allele. *ht incomp*, heterogametic incompatibility; *ho incomp*, homogametic incompatibility.

is affected (Figure 1a). Obviously, unidirectional X–A heterogametic incompatibility is a much weaker selection than a homogametic one. In the case of compound ($X_1A_2 + X_2B_1$) bidirectional incompatibilities when A_2 and B_1 are localized on different autosomes and H_1 and H_2 are equally mixed, the equilibrated L approaches 1.000 under the condition of either heterogametic or homogametic incompatibilities (Figure 1b).

Heterogametic and homogametic incompatibilities also display differential influences on allele frequencies in such an enclosed deme. The allele frequencies are the functions of fitness ($W^{(t)}$) and time (generation t) (Equation (10)). Figure 2 shows the allele frequencies in such a static admixture deme in generation t in the presence of a unidirectional, sex-biased hybrid X_1A_2 incompatibility. In this scenario, P_{X1}, the frequency of the incompatible allele X_1, is rapidly reduced to zero in both heterogametic and homogametic incompatibilities (Figure 2a). P_{A1}, the frequency of the compatible allele at the A locus (here, the incompatible allele is A_2), reaches equilibrium at 0.67 when the heterogametic sex is affected and 0.80 when the homogametic sex is affected (Figure 2c). P_{C1}, the frequency of the neutral, autosomal allele C_1 that is not related to a genetic incompatibility, equilibrates at 0.493 when the heterogametic sex is affected and 0.476 when the homogametic sex is affected (Figure 2d). Here, the B locus is not involved in incompatibility and behaves the same as 'C' at the moment. With the exception of the Y locus (Figure 2b) that is not selected under a homogametic incompatibility, the frequencies of all alleles in the deme shift away from their initial ratio of 0.5:0.5. The establishment of equilibrium of allele frequencies in a closed deme under a sex-biased incompatibility takes several generations.

We then consider a chain of static demes, each of which receives initial contributions from two parental populations with an H_1:H_2 ratio gradually changing from 1:0 to 0:1, again with zero dispersal in the following generations. As shown in Figure 3, L distributions (an indicator of intrinsic strength of genetic selection) in these demes display obvious asymmetry. An X_1A_2 heterogametic incompatibility is a more polarizing and a much weaker barrier (Figure 3). Changes in allele frequencies across these demes again show differences between heterogametic and homogametic incompatibilities. Figure 4a shows the plots of allele frequencies in a chain of demes. Here, a straight, diagonal distribution of allele frequency suggests that a locus is not directly selected against by the incompatibility, as shown by the straight diagonal distributions of P_{Y1} in Figures 4a and b. However, an 'S'-shaped distribution would suggest stronger selection. A distribution that passes the geometric center of each plot would suggest symmetric selection.

Using a static admixture model, intrinsic differences between heterogametic and homogametic genetic selection are demonstrated. If one puts such a chain of demes in a hybrid zone and considers dispersal, this model can be used to analyze the hybrid zone dynamics. We consider here both long-range (see Asmussen *et al.*, 1989; Orive and Barton, 2002) and short-range dispersal (Endler, 1973; Orive and Barton, 2002). For long-range dispersal, the hybrid zone consists of 10 demes and each deme receives inputs proportional to its relative distance from either parental population. It is assumed that, in every generation, each deme loses 1% of its offspring to migration and, at the same time, receives inputs from both parental populations equal to 1% of the deme's maximum size. For short-range dispersal, we adopt the stepping stone model (Endler, 1973), in which migrations occur only between adjacent demes. The hybrid zone consists of 10 demes. In every generation, each deme

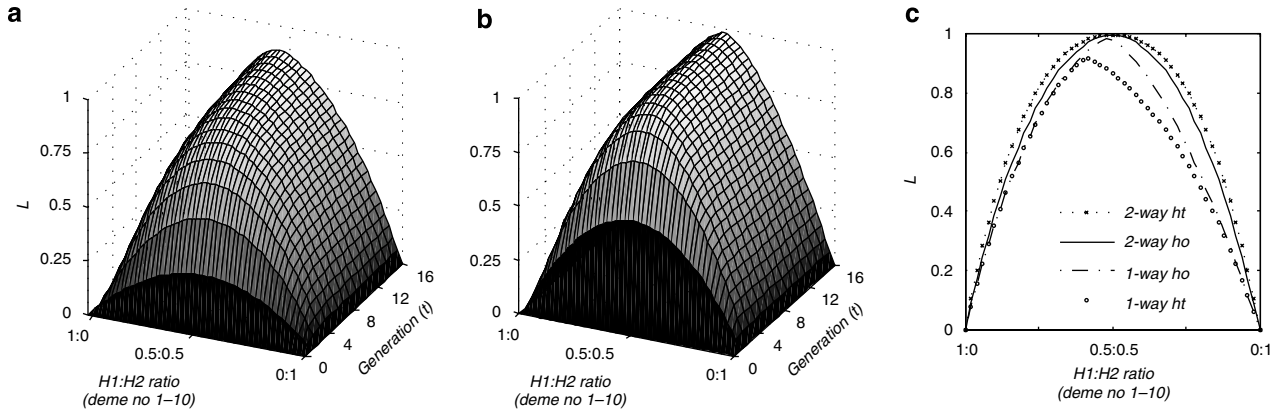

Figure 3 The genetic load (L) in a chain of demes with gradually changing contributions from parental populations ranging from 1:0 to 0:1 in the presence of X–A sex-biased incompatibilities. (**a**) L under the unidirectional X_1A_2 heterogametic incompatibilities; (**b**) L under the unidirectional X_1A_2 homogametic incompatibilities; (**c**) L of the different unidirectional or bidirectional incompatibilities after equilibration is established. *2-way ht*, compounding bidirectional heterogametic incompatibilities; *2-way ho*, compounding bidirectional homogametic incompatibilities; *1-way ho*, unidirectional homogametic incompatibility; *1-way ht*, unidirectional heterogametic incompatibility.

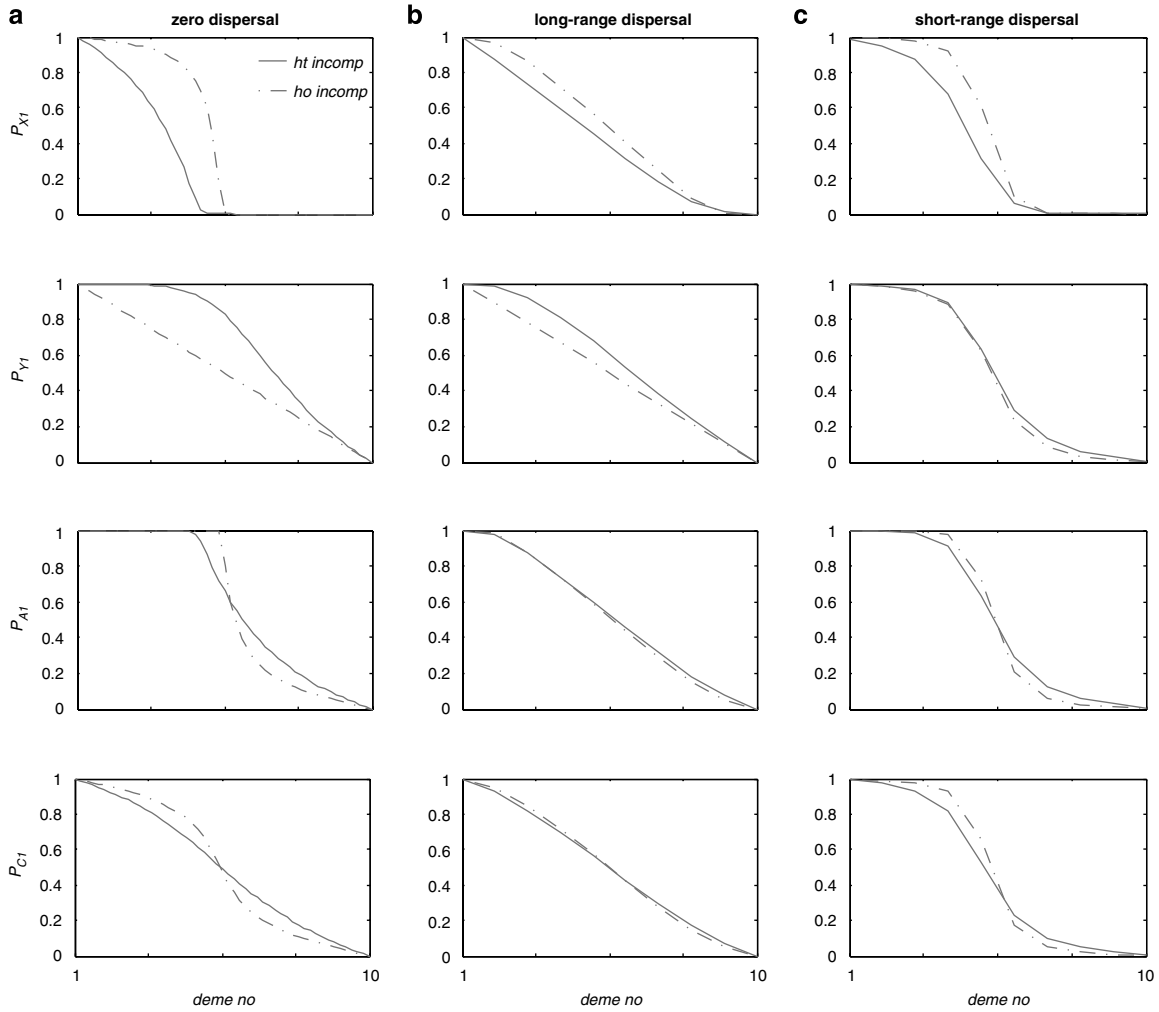

Figure 4 The distribution of allele frequencies (P) across a zone that consists of a chain of 10 demes in the presence of unidirectional X_1A_2 sex-biased hybrid incompatibility. (**a**) A scenario with zero dispersal; here, demes receive parental contributions once, H_1:H_2 gradually changes from 1:0 to 0:1. (**b**) A scenario with long-range dispersal at a rate $\lambda = 0.01$. In each generation, each deme receives inputs from both parental populations equal to 1% of the deme's maximum size and, at the same time, loses 1% of its offspring to migration. (**c**) A scenario with short-range dispersal at a rate $\lambda = 0.4$. Each deme receives 20% of migrants from the adjacent deme on each side and loses 40% of the individuals to the adjacent demes (20% on each side). Here, B locus is not involved in the incompatibility and thus B_1 would behave like the C_1 allele. *ht incomp*, heterogametic incompatibility; *ho incomp*, homogametic incompatibility.

loses 40% (20% to each side) of its offspring to migration and, at the same time, receives inputs of 20% from the adjacent deme on each side. The end demes on both sides of the zone exchange migrants with the corresponding parental populations. Figures 4a, b and c present allele frequencies across a hybrid zone with zero, long-range and short-range dispersal, respectively.

It can be seen that the spatial patterns of the clines of different loci differ from each other. *X* and *A* clines are narrower than that of a neutral '*C*', the part of the genome not under direct selection and the representation of overall selection strength. A unidirectional X_1A_2 incompatibility is a characteristic asymmetrical mechanism, with the *X* cline moving toward H_1 and the '*A*' cline moving toward H_2. The P_{C1} value under a heterogametic X_1A_2 incompatibility displays a relatively more diagonal distribution (Figure 4), suggesting that the heterogametic X_1A_2 incompatibility is a weaker barrier than a homogametic one. A sex-biased incompatibility in a hybrid zone with 1% long-range dispersal appears to be a poor barrier. All allele frequencies in this scenario show more diagonal distributions (Figure 4b), compared with those in the scenario of 40% short-range dispersal (Figure 4c). Such a trend of diagonal distributions is more obvious, when long-range dispersal is larger at 10% (data not shown). It is also noteworthy that the trends of allele frequencies are similar in all three scenarios of dispersal, except for relative width and steepness of each cline. The trend of differentiation between heterogametic and homogametic incompatibilities is also the same. Understandably, the time required to establish equilibrium is longer in cases with dispersal. This analysis indicates that the case with zero dispersal is a good representation of the differentiations between heterogametic and homogametic incompatibilities.

The same analysis with zero dispersal was also applied to other sex-biased incompatibilities, that is, the *X*–*Y* heterogametic incompatibilities, *Y*–*A* heterogametic incompatibilities' *X*–*X* homogametic incompatibility, autosomal–autosomal (*A*–*B*, where *A* and *B* are unlinked independent autosomal loci) heterogametic incompatibility, and autosomal–autosomal (*A*–*B*) homogametic incompatibility. Figure 5 shows the P_{C1} distributions in the static model, representing the intrinsic selection strength of these barriers against neutral gene flow. Again, all the unidirectional, sex chromosome-linked and sex-biased hybrid incompatibilities exhibit differential strengths and patterns of selection. The heterogametic *X*–*Y* and *Y*–*A* incompatibilities are much milder mechanisms (Figure 5a), as is the heterogametic X_1A_2 incompatibility (Figure 4a), in which P_{C1} exhibits a more diagonal distribution. Interestingly, unidirectional, heterogametic *A*–*B* and homogametic *A*–*B* incompatibilities exhibit an identical P_{C1} distribution (Figure 5b) and both of them are stronger isolating barriers than heterogametic incompatibilities linked to a sex chromosome.

The compound $X_1A_2 + X_2B_1$ bidirectional incompatibilities were analyzed, in which *A* and *B* are independent/unlinked autosomal loci. Hybridization of both directions causes inferiority in either the heterogametic or homogametic sex. Such compound heterogametic incompatibilities are often found in instances of Haldane's rule. Analysis indicates that both compound heterogametic and homogametic incompatibilities are

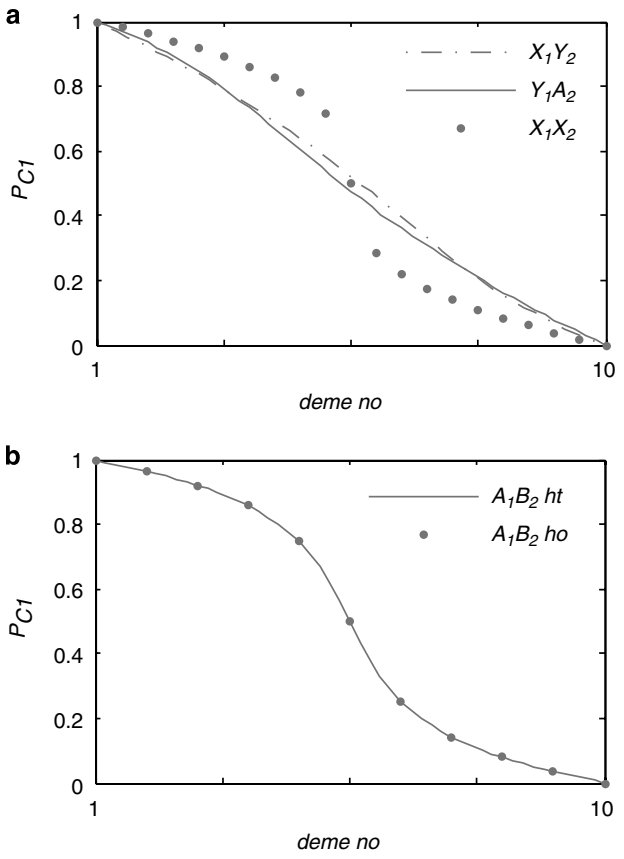

Figure 5 The frequency distribution of a neutral allele (P_{C1}) across a hybrid zone in the presence of other forms of sex-biased incompatibilities. The hybrid zone consists of a chain of demes with gradually changing parental contributions ranging from 1:0 to 0:1. (**a**) X_1Y_2 and Y_1A_2 heterogametic incompatibilities, and X_1X_2 homogametic incompatibility; (**b**) A_1B_2 heterogametic and A_1B_2 homogametic autosome-linked incompatibilities. *ht*, heterogametic incompatibility; *ho*, homogametic incompatibility.

stronger isolation. The compound heterogametic incompatibility ($X_1A_2 + X_2B_1$) is somewhat a wider and stronger barrier against gene flow across a hybrid zone (Figure 3c). In an equal admixture (H_1:H_2 = 1:1), the equilibrated *L* approaches 1.000 under the condition of either heterogametic or homogametic incompatibilities (Figures 1b and 3c). The difference between unidirectional and bidirectional heterogametic incompatibilities ($L \approx 0.867$ vs $L \approx 1.000$) is larger than that between homogametic incompatibilities ($L \approx 0.982$ vs $L \approx 1.000$; Figures 1b and 3c) when the contributions from the parental populations are at a 0.5:0.5 ratio. A stronger selection of compound heterogametic incompatibilities and a larger stepwise increase from unidirectional to compound bidirectional heterogametic incompatibilities are consistent with what was found in the introgression model (Wang, 2003).

If one looks at the allele frequencies in a chain of demes with gradually changing parental contributions from 0:1 to 1:0, both compound bidirectional incompatibilities are less polarizing barriers in which only *A* and *B* loci are under asymmetrical selection (Figure 6). The *X* cline under the compound bidirectional incompatibilities is extremely narrow, which is the only locus where heterogametic and homogametic incompatibilities

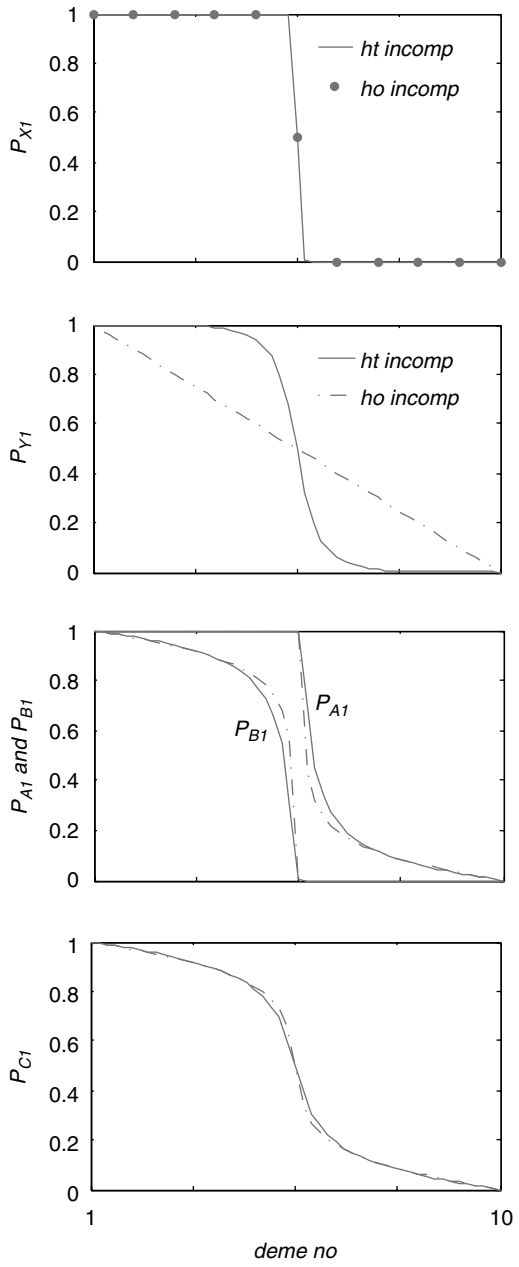

Figure 6 The distribution of allele frequencies (P) across a hybrid zone that consists of a chain of demes with gradually changing H_1:H_2 contributions ranging from 1:0 to 0:1 in the presence of compound bidirectional $X_1A_2 + X_2B_1$ sex-biased hybrid incompatibility. *ht incomp*, heterogametic incompatibility; *ho incomp*, homogametic incompatibility.

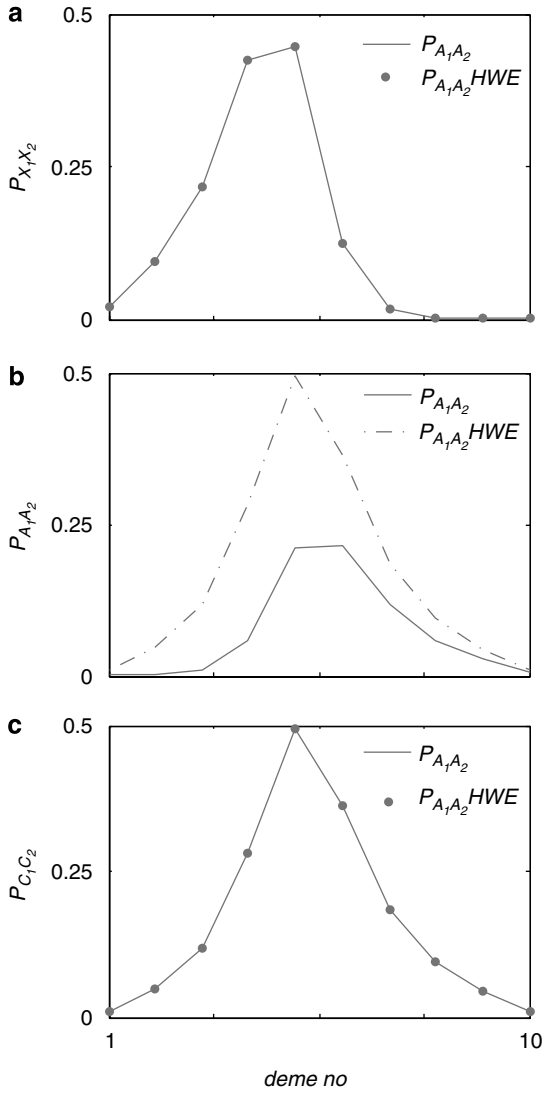

Figure 7 Comparison of genotype distributions predicted by the current model and the Hardy–Weinberg equation. (**a**) X_1X_2 distribution, (**b**) A_1A_2 distribution and (**c**) C_1C_2 distribution in a hybrid zone maintained by a unidirectional X_1A_2 heterogametic incompatibility and short-range dispersal with $\lambda = 0.4$ (see text and Figure 4c for details). Equations (4) and (5) are used to calculate the genotype distributions. 'X_1X_2 *HWE*', 'A_1A_2 *HWE*', and 'C_1C_2 *HWE*' are the genotype distributions predicted by the Hardy–Weinberg equation using the allele frequencies shown in Figure 4c.

display almost identical frequency distributions (Figure 6). The clines of different loci differ in their widths, shapes and asymmetry. The clines of incompatible alleles are narrower, suggesting that these alleles face stronger introgression constraint than others.

To assess how a sex-biased hybrid incompatibility can influence genotype distributions, we compared the frequencies of representative genotypes in a hybrid zone with those predicted by the Hardy–Weinberg equilibrium. Figure 7 presents X_1X_2, A_1A_2 and C_1C_2 frequencies in a hybrid zone maintained by an X_1A_2 heterogametic incompatibility and short-range dispersal ($\lambda = 0.4$). For comparison, genotype distributions predicted by the Hardy–Weinberg equation are also plotted in Figure 7 (based on frequencies shown in Figure 4c). It was found that all three genotypes show deviation from the Hardy–Weinberg predictions in a hybrid zone maintained by an X_1A_2 heterogametic incompatibility. The A_1A_2 hybrids show the largest departure. A much smaller fraction of A_1A_2 hybrids was found in the center of such a hybrid zone than the Hardy–Weinberg prediction. Distributions of X_1X_2 and C_1C_2 show very small shifts from the Hardy–Weinberg expectations. In Figures 7a and c, their distributions almost overlap because the scales used are too large to show the differences. It will be interesting to see whether such distribution patterns are followed in natural hybrid

zones. In a scenario when an X_1A_2 heterogametic incompatibility indeed acts as a main force in maintaining a hybrid zone, one could expect a similar distribution of these three genotype frequencies. Such empirical tests will help assess the contribution of heterogametic incompatibility to population dynamics and also the feasibility of the current model.

Discussion

In this paper, we present a model of hybrid zones maintained by sex-biased BDM incompatibilities. Our analysis suggests that heterogametic and homogametic incompatibilities impose differential genetic selection in hybrid zones. These two barriers do differ in their selection strengths and patterns, and affect divergence differently. Comparing with a homogametic incompatibility or autosomal-linked incompatibility, a heterogametic incompatibility is a weaker and more asymmetric barrier, resulting in clines with distinct structure features. These features can be used for testing the feasibility of the current model in the field. The comparison between heterogametic and homogametic incompatibilities is consistent with what was found in an introgression model, which showed discrepancies owing to the zygosity of the *X* and *Y* chromosomes (Wang, 2003). The most noted is the mildness of unidirectional heterogametic incompatibilities. Compared with other forms of sex-biased BDM incompatibilities (such as *X–A* homogametic incompatibility, autosomal–autosomal homogametic incompatibility and autosomal–autosomal heterogametic incompatibility), a sex chromosome-linked BDM heterogametic incompatibility (*X–A* or *X–Y* or *Y–A* heterogametic incompatibility) is always unidirectional. It usually affects F_1 offspring in one direction of hybridization but not in the reciprocal direction, whereas all other mechanisms will affect F_1 offspring in both directions (for details, see also Wang, 2003). The unidirectionality of single heterogametic incompatibilities appears to lead to milder isolation.

Whether differences between heterogametic and homogametic incompatibilities could lead to prevalent preservation or presence of heterogametic incompatibilities during speciation is not clear. Nonetheless, the current model and its analytical results provide some useful insights into the dynamics of hybrid zones where a sex-biased incompatibility is present. One could expect that this diversity of population dynamics (quantitative differences between heterogametic and homogametic incompatibilities) will influence local adaptation and collapse/extinction of populations. Populations with partial isolation could face one of the following fates: remain in partial isolation, diverge further to become full species or collapse into a single population. Haldane's rule would be produced if the populations with heterogametic incompatibilities tend to remain partially isolated, while those with homogametic incompatibilities tend to collapse or rapidly become more complete species. In other words, evolutionary dynamics may make heterogametic incompatibility more visible in nature than homogametic ones. If this is the case, all BDM incompatibilities affecting the heterogametic sex would have similar chances to be observed, whether they are *X*-linked recessivity, *XA* translocation, meiotic drive, disrupted dosage compensation or other sex chromosome-linked incompatibilities.

If a heterogametic incompatibility can indeed prolong its own presence and visibility because of population dynamics, it would have more influence on genome divergence through partial gene flow. Gene flow may be strongly blocked in some regions, such as the regions closely linked to X_1 and A_2 in the presence of an X_1A_2 incompatibility and to X_1, A_2, X_2 and B_1 in $(X_1A_2 + X_2B_1)$ bidirectional incompatibilities, but much less affected in other regions, such as the neutral C regions. The restricted loci tend to have narrower and steeper clines (see P_{X1}, P_{A1} in Figure 4 and P_{X1}, P_{A1}, P_{B1} in Figure 6), but neutral ones have wider and less steep clines (see P_{C1} in Figures 4 and 6). Such uneven gene flow may produce unique genomic signatures, that is, faster divergence of the *X* and some autosomal regions (*A* and/or *B*) of the genome, which appears to be consistent with empirical observations (Charlesworth *et al*., 1987; Wang *et al*., 1997; Torgerson and Singh, 2006). By dissecting and tracing patterns of genomic divergence, one may thus decipher the genetic mechanisms driving speciation. The population dynamics constraining the exchange of *X* alleles might also account for faster evolution of species with larger *X* chromosomes (Turelli and Begun, 1997) because an *X* locus is more likely on a faster track of divergence. Sub-populations in a metapopulation with such selective, uneven gene flow could enjoy a relative independence for the benefit of local adaptation and, at the same time, share advantageous mutations through limited gene flow. This notion is in agreement with the high genetic similarity between many distinct species that are not separated by strong physical barriers, such as those observed in *Drosophila* (Ranz *et al*., 2003), birds (Crochet *et al*., 2003; Lijtmaer *et al*., 2003) and Lepidoptera (Presgraves, 2002). Given the prevalence of Haldane's rule, sex-biased genetic incompatibilities could be a major driving force behind such genomic divergence. Ongoing sequencing project on closely related species of *Drosophila melanogaster* subgroup, including *D. simulans*, *D. sechellia* and *D. mauritiana* in comparison with *D. melanogaster* and other related species, may provide valuable insights in this regard.

Acknowledgements

We thank Jonathan Sheps, Timothy Vines, Cortland Griswold, the editor and four anonymous reviewers for their constructive comments in writing and revising the manuscript. We thank Melvin Kwok for technical support. We also thank Victor Ling for financial assistance.

References

Asmussen MA, Arnold J, Avise JC (1989). The effects of assortative mating and migration on cytonuclear associations in hybrid zones. *Genetics* **122**: 923–934.

Barton N, Bengtsson BO (1986). The barrier to genetic exchange between hybridising populations. *Heredity* **57**: 357–376.

Barton NH (1979). Gene flow past a cline. *Heredity* **43**: 333–339.

Barton NH (1980). The hybrid sink effect. *Heredity* **44**: 277–278.

Barton NH (1986). The effects of linkage and density-dependent regulation on gene flow. *Heredity* **57**: 415–426.

Bengtsson BO (1985). The flow of genes through a genetic barrier. In: Greenwood JJ, Harvey PH, Slatkin M (eds).

Evolution: Essays in Honour of John Maynard Smith. Cambridge University Press: Cambridge, UK, pp 31–42.
Charlesworth B, Coyne JA, Barton NH (1987). The relative rates of evolution of sex chromosomes and autosomes. *Am Nat* **130**: 113–146.
Cline TW, Meyer BJ (1996). Vive la difference: males vs females in flies vs worms. *Annu Rev Genet* **30**: 637–702.
Coyne JA, Orr HA (1989). Two rules of speciation. In: Otte D, Endler JA (eds). *Speciation and its Consequences*. Sinauer Associates: Sunderland, MA, pp 180–207.
Crochet PA, Chen JZ, Pons JM, Lebreton JD, Hebert PD, Bonhomme F (2003). Genetic differentiation at nuclear and mitochondrial loci among large white-headed gulls: sex-biased interspecific gene flow? *Evolution* **57**: 2865–2878.
Dobzhansky TG (1937). *Genetics and the Origin of Species*, 2nd revised edn. Columbia University Press: New York, xviii, 446pp incl. illus., Tables, diagrs.
Endler JA (1973). Gene flow and population differentiation. *Science* **179**: 243–250.
Frank SA (1991). Divergence of meiotic drive-suppression systems as an explanation for sex-biased hybrid sterility and inviability. *Evolution* **45**: 262–267.
Gavrilets S (1997). Hybrid zones with Dobzhansky-type epistatic selection. *Evolution* **51**: 1027–1035.
Haldane JBS (1922). Sex-ratio and unisexual sterility in hybrid animals. *J Genet* **12**: 101–109.
Haldane JBS (1932). *The Causes of Evolution*. Longmans Green and Co.: London, New York, vii, 234 pp.
Heikkinen E, Lumme J (1998). The Y chromosomes of *Drosophila lummei* and *D. novamexicana* differ in fertility factors. *Heredity* **81**: 505–513.
Hurst LD, Pomiankowski A (1991). Causes of sex ratio bias may account for unisexual sterility in hybrids: a new explanation of Haldane's rule and related phenomena. *Genetics* **128**: 841–858.
Laurie CC (1997). The weaker sex is heterogametic: 75 years of Haldane's rule. *Genetics* **147**: 937–951.
Lijtmaer DA, Mahler B, Tubaro PL (2003). Hybridization and postzygotic isolation patterns in pigeons and doves. *Evolution* **57**: 1411–1418.
Muller HJ (1940). Bearings of the '*Drosophila*' work on systematics. In: Huxley JS (ed). *The New Systematics*. Clarendon: Oxford, pp 185–268.
Muller HJ (1942). Isolating mechanisms, evolution and temperature. *Biol Symposia* **6**: 71–125.
Nagylaki T (1975). Conditions for the existence of clines. *Genetics* **80**: 595–615.
Orive ME, Barton NH (2002). Associations between cytoplasmic and nuclear loci in hybridizing populations. *Genetics* **162**: 1469–1485.
Orr HA (1993a). Haldane's rule has multiple genetic causes. *Nature* **361**: 532–533.
Orr HA (1993b). A mathematical model of Haldane's rule. *Evolution* **47**: 1606–1611.
Pantazidis AC, Galanopoulos VK, Zouros E (1993). An autosomal factor from *Drosophila arizonae* restores normal spermatogenesis in *Drosophila mojavensis* males carrying the *D. arizonae* Y chromosome. *Genetics* **134**: 309–318.
Pantazidis AC, Zouros E (1988). Location of an autosomal factor causing sterility in *Drosophila mojavensis* males carrying the *Drosophila arizonensis* Y chromosome. *Heredity* **60** (Part 2): 299–304.
Presgraves DC (2002). Patterns of poszygotic isolation in Lepidoptera. *Evolution* **56**: 1168–1183.
Ranz JM, Castillo-Davis CI, Meiklejohn CD, Hartl DL (2003). Sex-dependent gene expression and evolution of the *Drosophila transcriptome*. *Science* **300**: 1742–1745.
Slatkin M (1973). Gene flow and selection in a cline. *Genetics* **75**: 733–756.
Torgerson DG, Singh RS (2006). Enhanced adaptive evolution of sperm-expressed genes on the mammalian X chromosome. *Heredity* **96**: 39–44.
Turelli M (1998). The causes of Haldane's rule. *Science* **282**: 889–891.
Turelli M, Begun DJ (1997). Haldane's rule and X-chromosome size in *Drosophila*. *Genetics* **147**: 1799–1815.
Turelli M, Orr HA (1995). The dominance theory of Haldane's rule. *Genetics* **140**: 389–402.
Turelli M, Orr HA (2000). Dominance, epistasis and the genetics of postzygotic isolation. *Genetics* **154**: 1663–1679.
Wang RL, Wakeley J, Hey J (1997). Gene flow and natural selection in the origin of *Drosophila pseudoobscura* and close relatives. *Genetics* **147**: 1091–1106.
Wang RX (2003). Differential strength of sex-biased hybrid inferiority in impeding gene flow may be a cause of Haldane's rule. *J Evol Biol* **16**: 353–361.
White MJD (1945). *Animal Cytology & Evolution*. University Press: Cambridge, 375pp.
Wu C-I, Davis AW (1993). Evolution of postmating reproductive isolation: the composite nature of Haldane's rule and its genetic bases. *Am Nat* **142**: 187–212.